RAD Conference Proceedings, vol. 5, pp. 104–109, 2021
ISSN 2466-4626 (online) | DOI: 10.21175/RadProc.2021.20
www.rad-proceedings.org

DEVELOPMENT OF AN MCNP MODEL OF A BORON-10 ZINC SULFIDE SILVER-ACTIVATED [^{10}B/ZnS(Ag)] DETECTOR AND DIRECTIONAL SHIELDING USING RADIATION COUNTING

Alexander Macris[1], Kevin McKay[1], William Charlton[1], Cheryl Brabec[2], Sheldon Landsberger[1*]

[1]University of Texas at Austin, Nuclear Engineering Teaching Laboratory, Austin, Texas, USA
[2]Los Alamos National Laboratory, Los Alamos, New Mexico, USA

Abstract. *For radiological neutron surveying, neutron detectors require shielding to minimize contributions from sources outside the area of interest. To test the effectiveness of such a shield, Monte Carlo N-Particle Transport Codes (MCNP) were used to model a neutron detector so that the effectiveness of such a shield design could be explored. In this research, MCNP models of a ^{10}B/ZnS detector within a shield were developed and compared to experimental results. By carefully modeling the specifics of the neutron detector as well as the neutron source used in the experiments, the simulation was able to accurately predict the experimental results within 20%.*

Key words: *Neutron detection, ^{10}B, MCNP*

1. INTRODUCTION

1.1. Purpose

At Los Alamos National Laboratory (LANL), workers must frequently perform radiological surveys of radioactive waste storage rooms. The large amount of radioactive material in the rooms coupled with the amount of time needed to perform the surveys could result in significant radiological exposure to workers. LANL hopes to develop a directionally sensitive shield assembly to surround a detector so that it can accurately measure radiation levels of individual containers by attenuating contributions from other sources within a room. This detector could then be attached to a robot so that it can perform the radiation surveys and minimize the dose received by workers.

In order to assess two different shield designs' ability to minimize counting contributions from sources outside of an area of interest, a Monte Carlo N-Particle Transport Code (MCNP) model of a boron-10 zinc sulfide (^{10}B/ZnS(Ag)) scintillation detector was developed. Experimental counts were then performed using a plutonium-beryllium (PuBe) neutron source placed at various locations around the detector. The PuBe source was then included in the MCNP model, and neutron reaction rates in the detector's active area were tallied to validate the model's results with the experimental measurements.

Experimental measurements were then performed with two PuBe sources and with the detector placed in two different directional shielding designs. Counts were recorded with one source remaining stationary in front of a window cut into the outer layer of the shield while the second was revolved around the detector. These counts were then used to analyze each shield's ability to minimize the counting contributions from the second source according to the source's location. Furthermore, these measurements were used to analyze the accuracy of the MCNP model of the detector when placed in both shielding designs.

Once validated, more complex distributions of sources can be included in the shielded detector models to better represent the layout of the waste storage rooms at LANL that the shielded detector will be sent into for radiological surveys. The results from these more complex models will then be used as a benchmark for the neutron measurements recorded for the waste items in the storage vaults.

1.2. Background

The ^{10}B/ZnS(Ag) detector from Bridgeport Instruments is a scintillation style neutron detector that relies on the alpha particles released from neutron capture reactions in the boron-10. The excited alpha particles deposit their energy in the zinc sulfide scintillator to produce visible light, which is converted into electronic pulses by a photomultiplier tube (PMT).

At one end of the detector, a Lucite acrylic cylinder serves as a light guide to transport the light to the PMT. This light guide also acts as an internal moderator, which helps increase the efficiency of the detector since the neutron capture reaction is more likely to occur with thermal neutrons [1]. The measured count rate can be increased further by surrounding the exterior of the detector with more moderating material.

The neutron sources used were two 1-Ci PuBe sources produced by Monsanto Research Corporation. Most neutrons produced from these sources result from the neutron emission caused by the absorption of the alpha particles from plutonium decay in ^{9}Be, with others coming from spontaneous fission in the plutonium. The total emission rate for one source, M797, was calibrated as 1.85×10^{6} ± 2.5% neutrons/second on Nov. 3, 1961.

* s.landsberger@mail.utexas.edu

The other source, M196, was calibrated with an emission rate of $1.62 \times 10^6 \pm 2.5\%$ neutrons/second on Aug. 22, 1961. Both PuBe sources have an outer stainless-steel casing and inner cladding made of tantalum that houses the plutonium-beryllium mixture. The initial calibration provided by the manufacturer for source M196 stated a plutonium and beryllium mass of 15.88 grams and 7.93 grams, respectively. M197 was initially calibrated with 15.97 grams of plutonium, of which 14.856 grams was ^{239}Pu, and 7.86 grams of beryllium.

The two shielding designs developed for the detector include concentric cylindrical layers of both absorbing and moderating materials. One design includes a 2.54 cm thick outer layer of high-density polyethylene (HDPe), a 0.0508 cm thick second layer of cadmium, and 2.54 cm thick innermost layer of borated polyethylene. The second design has the same dimensions and materials but differs in that the borated polyethylene is the outermost layer, followed by the cadmium, and HDPe layers. Both designs include a bottom endcap that is composed of the material that makes up their respective innermost layer. A window is then cut through the outermost layer so that there is less attenuating material between the detector and a source in front of the opening. This allows for more neutrons passing through the window to reach the detector while those coming from outside the area are attenuated by the shielding. Both shielding designs can be seen below in Figure 1.

Figure 1. Two Directional Shielding Designs with Concentric Layers of Borated Polyethylene, Cadmium, and HDPe.

2. Experimental

The neutron measurements were performed in a large concrete room at the Nuclear Engineering Teaching Lab at the University of Texas at Austin.

The first counts recorded were with only source M196 placed 63.5 cm (25 inches) in front of the detector face with a borated polyethylene housing placed around the detector. The borated polyethylene housing around the detector can be seen below in Figure 2. The source was then revolved around the detector at intervals of 15° with respect to the detector face at a constant distance of 63.5 inches. The purpose of recording measurements at each angle was to evaluate how the recorded counts changed according to the angular location of the source. These measurements at each angle, which can be seen in Figure 3, were then modelled in MCNP to evaluate whether the detector model was accurate for multiple source locations. A background count was also recorded with the detector placed in the borated polyethylene housing, but the background was considered negligible because the count rate was on the order of one count per 1000 seconds.

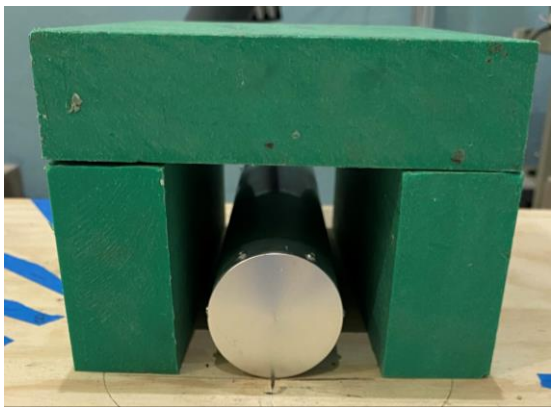

Figure 2. ^{10}B/ZnS(Ag) Detector Placed in Borated Polyethylene Housing.

The purpose of the borated polyethylene housing was to minimize the counting contributions from neutrons that scattered off miscellaneous items within the room and back towards the detector. The empty space between the blocks and the detector do not pose a problem for neutron detection. The various objects in the room would be very difficult to include in the MCNP model, so having the absorbing material helped limit the neutrons reaching the detector to those coming directly from the source, which is more accurate for comparison to the results given by the MCNP models. These measurements were used as a benchmark for the MCNP model without the LANL shield around it to ensure that our model of the detector does not depend on the LANL shield.

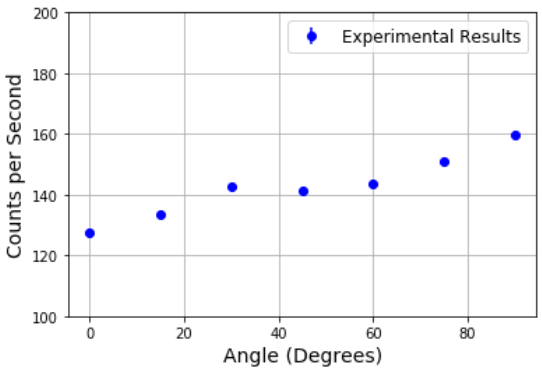

Figure 3. Measured Count Rate for Source M196 Located at Various Angles with Detector Placed in Borated Polyethylene Housing.

Error bars are present in Figure 3; however, they are too small to be seen as the uncertainty was assumed using only counting statistics with the uncertainty being the square root of the total counts divided by the counting time. This will be the case for all experimental measurements taken. The real uncertainty is higher than this approximation due to factors such as room return neutrons, but this uncertainty cannot be known precisely.

As seen in Figure 3, the measured count rate increased as the source was rotated towards the side of the detector. This is due to both the inner geometry of the detector and the borated polyethylene housing. The active detecting element is a thin layer of the ^{10}B/ZnS(Ag) mixture deposited around the curved portion of the cylindrical Lucite light guide. As the source moved toward the side of the detector, the effective surface area of the detector increased due to the source being located more directly in front of the detecting layer. Furthermore, as the source was moved towards the side of the detector, more neutrons passed through the borated polyethylene housing. The large amount of hydrogen in the polyethylene moderated the incident fast neutrons, which make up most of the neutron spectrum from PuBe sources [2]. This increased the likelihood that they would be absorbed in the detector's active layer due to ^{10}B having a higher absorption cross-section for thermal neutrons.

The next set of measurements were performed with the detector placed within the cylindrical directional shields pictured in Figure 1 and with both PuBe sources present. This experimental setup is pictured below in Figure 4. The borated polyethylene housing was not needed for these measurements because the cylindrical shields provided the attenuation for scattered neutrons.

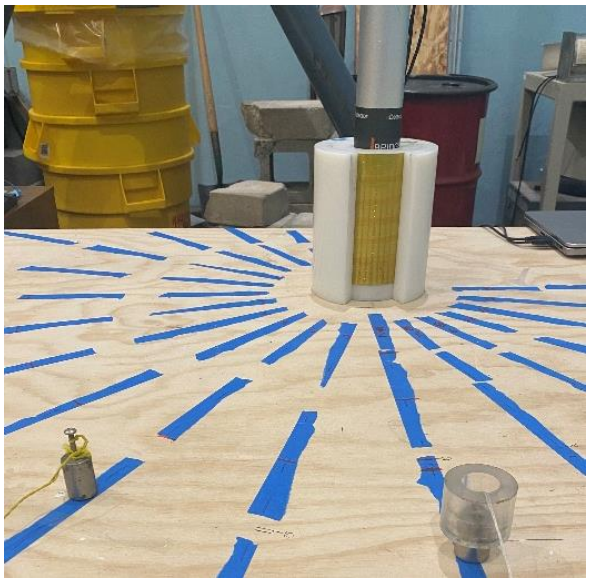

Figure 4. ^{10}B/ZnS(Ag) Detector Placed in Directional Shield with Source M196 Located in Front of Shield Window and Source M797 Offset by 30°.

Background counts were performed again with the detector placed in both shielding designs prior to introducing the PuBe sources. The measured background proved to be negligible as the count rate was on the order of 0.001 cps.

Counts were then recorded with source M196 placed directly in front of the shield window at 63.5 cm (25 in.) from the center of the detector. These counts served as the baseline for the expected number of counts from source M196 since there were no outside sources present. Source M797 was then placed alongside source M196 in front of the shield window. Starting at this position, source M797 was revolved around the detector at intervals of 15° with respect to the center of the detector at a constant distance of 63.5 cm, while source M196 remained at its position in front of the shield window. The inclusion of two sources in the experiment served to simulate the shields' desired directional applications and compare the shields' effectiveness at minimizing the counting contributions from outside sources. The experimental results were also used to verify the accuracy of the MCNP model of the detector when placed in the shielding.

After performing measurements with the detector placed in the cylindrical shields, the same procedure was done with the detector standing vertically, like in Figure 4, but with no shielding present. While these measurements were not used to compare to the MCNP models, they were used to assess the effects each shield had on the measured count rates.

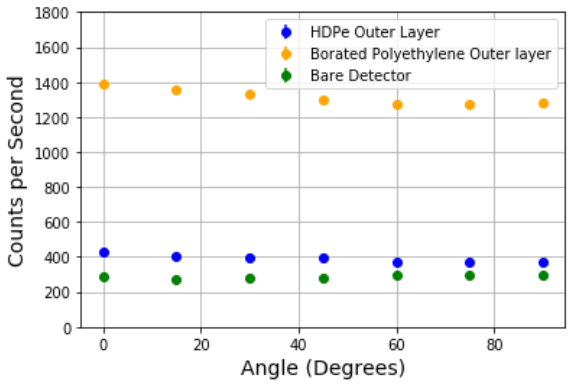

Figure 5. Neutron Count Rate Comparison Between Unshielded and Shielded Detector Setups According to the Angular Location of Source M797.

As seen in Figure 5, the count rates were lower at each angle for the unshielded detector than they were for both shielded detectors. This is because the efficiency of the detector increases in the presence of moderating material due to the ^{10}B in the detector being more likely to absorb slower neutrons. So, without any shielding placed around the detector, most of the fast neutrons born from the PuBe sources pass through the detector without being detected.

The purpose of the cylindrical shielding designs was to attenuate only the neutrons coming from sources located outside of the area in front of the shield window so that accurate measurements could be made of a source in front of it. In analyzing the results in Figure 5, one sees that the neutron count rate decreases as source M797 is moved away from the window for both shields whereas it begins to increase for the unshielded detector. The decrease in counts is caused by an increase in the amount of shielding outside of the window due to the presence of the outer layer. So, as the solid angle between source M797 and the window decreases, more neutrons must travel through all three layers of shielding to reach the detector.

To compare both shields' ability to limit the counting effects of the second source on the measurement of the first in front of the window, the ratio of counts recorded with both sources present to the number of counts measured from just source M196 are listed below in Table 1. With only one source placed in

front of the detector, the count rates were measured to be 183.5 cps ± 0.7% and 604.3 cps ± 0.4% for the designs with HDPe and borated polyethylene as the outer layer, respectively. For the unshielded detector, the count rate with one source was 124.15 cps ± 0.82%. Table 1 shows the ratio of the counts recorded with both sources present to the counts recorded with only one source present at a fixed location in front of the shielding window. The angle represents the location of the second source relative to the center of the detector, with 0° located directly in front of the window in the shielding design, as shown in Figure 4. At each angle, the sources are 25" away from the center of the detector.

Table 1. Ratios of Count Rates Measured with Two Sources Present Versus One Source for Different Locations of the Second Source.

Angle	Borated HDPe Ratio	HDPe Ratio	Unshielded Ratio
0°	2.30 ± 0.44%	2.32 ± 0.81%	2.30 ± 0.98%
15⁰	2.25 ± 0.45%	2.21 ± 0.81%	2.19 ± 0.99%
30⁰	2.20 ± 0.45%	2.16 ± 0.82%	2.25 ± 0.98%
45⁰	2.15 ± 0.45%	2.14 ± 0.82%	2.27 ± 0.98%
60⁰	2.11 ± 0.45%	2.03 ± 0.82%	2.36 ± 0.98%
75⁰	2.11 ± 0.45%	2.03 ± 0.82%	2.36± 0.98%
90⁰	2.12 ± 0.45%	2.03 ± 0.82%	2.39 ± 0.98%

The shield with the HDPe outer layer was more effective at attenuating the neutrons from the second source. The HDPe moderates the incident fast neutrons, increasing the likelihood that they are absorbed in the cadmium and borated polyethylene layers. This is due to both borated polyethylene and cadmium having higher absorption cross-sections for lower energy neutrons. For the other shield, the borated polyethylene serving as the outer layer minimized its ability to absorb neutrons because there was no moderating material to slow down the fast neutrons from the PuBe source. While the borated polyethylene did provide moderation for the neutrons to be absorbed in the inner layers, the HDPe in the innermost layer is not as effective of an absorber of neutrons due to its lower absorption cross-section.

While both shields' ability to attenuate neutrons from the second source improved as it was moved away from the window, neither shield was able to get the recorded counts back to near the initial value recorded with one source. As seen in Table 1, the ratio of counts recorded with two sources to those measured with one leveled out at 60° and was never reduced to less than two. This is partly because the second source, M797, has a higher source strength than M196, but it is also due to an insufficient amount of moderating material outside of the shielding window. ^{113}Cd, which makes up 12.2% of natural cadmium, has an extremely high thermal absorption cross-section of 20, 600 barns, but this value drops off very quickly as energy increases above the cadmium cutoff energy of ~0.7 eV [3]. By increasing the amount of moderating material, more neutrons will reach thermal energies and be absorbed in the cadmium layer of the shield.

3. MCNP Modeling

MCNP 6.2 was used for all simulations. Based on the specifications given by the manufacturer, the MCNP model of the detector, pictured inside a shielding design in Figure 6, includes an active area composed of Lucite coated with a thin layer of a ^{10}B zinc sulfide mixture, a PMT, and a thin aluminum casing [1]. While the surface density of the boron-10 was specified to be 1.8 mg/cm^2, the exact thickness of the detecting layer was not specified. A thickness of 0.17 cm was assumed based on the detecting elements found in other types of neutron scintillation detectors [4]. Information from the manufacturer of the detector implied the existence of an additional moderator between the boron detecting layer and the casing, and we chose this to be Lucite, the same material that composes the light guide. The PMT that makes up most the detector's internal volume was modeled as a volume of air, aluminum, and glass (Si_2O). Because aluminum and silicon have similar interaction cross-sections with neutrons, both on the order of 10^{-5} barns in the primary energy range of the source (~1 MeV), the cell containing the PMT was chosen to be aluminum with a modified density of 0.625 g/cm^3 [2] [5]. Oxygen possesses a higher interaction cross section of approximately 10^{-4} barns. However as there is twice as much silicon in the glass and the neutrons already have such a low interaction probability in the PMT, this was neglected. The aluminum density is that which provides enough mass to meet the mass specification provided by Bridgeport Instruments and is significantly lower than that of unaltered aluminum. All densities and compositions of materials used in this project are taken from Pacific Northwest Laboratory's materials compendium [6].

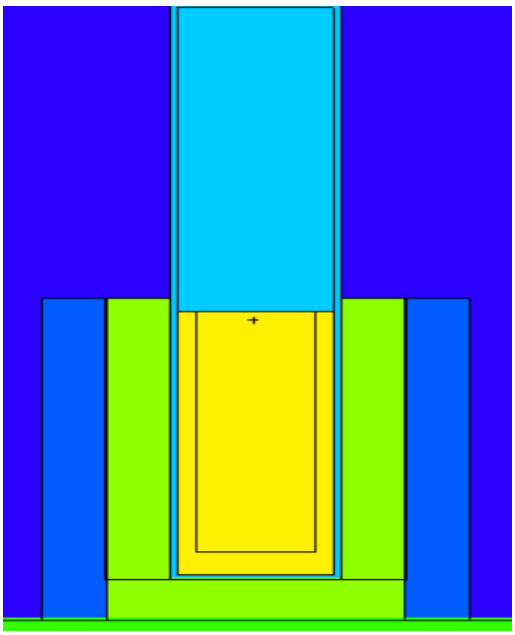

Figure 6. Detector model inside of the vertical shielding design.

To account for some of the neutron scatters occurring from objects in the room, the model also includes the concrete floor and walls, as well as the wooden table and plywood that the experimental setup sits on.

Lastly, the two neutron sources are characterized by the energy spectrum of a PuBe isotopic neutron source [7]. The sources' geometries are defined by an outer stainless-steel container, an inner tantalum cladding, and the plutonium beryllium mixture with the composition given by the manufacturer. The source in the MCNP model was defined as a uniformly distributed cylinder within the cell containing the plutonium-beryllium mixture. The code also includes both alpha-neutron reaction neutrons and spontaneous fission neutrons.

Since the calibrated source strengths given by the manufacturer were from the number of neutrons exiting the source container and not the number of neutrons being emitted directly inside the plutonium-beryllium mixture, flux tallies were measured in MCNP on the surface of both source casings to find the fraction of neutrons that exit the source. The result was that 1.4 times as many neutrons were exiting both source casings than were born within the PuBe source cell due to neutrons being emitted from induced fissions in the plutonium. Thus, the modified source strengths used for the MCNP calculations were the calibrated emission rates divided by 1.4.

Average flux (f4) tallies were then measured in the cell containing the thin layer of the ^{10}B and zinc sulfide mixture, and the resultant F4 tally was modified by a multiplier card to measure the number of neutron absorptions occurring in the ^{10}B per source particle [8]. This result was then multiplied by the modified neutron emission rates of the sources to get the number of absorptions occurring per second in the ^{10}B detecting layer, which is analogous to the count rate.

To check the accuracy of the detector model itself, without the effects of the LANL shield, simulations were performed with it laying horizontally within the borated polyethylene housing pictured in Figure 3. Source M196 was placed 25" from the face of the detector and then rotated about the face at this constant distance of 25" in increments of 15°. These results are shown in the graph in Figure 7. The count times for each angle were 120 seconds each.

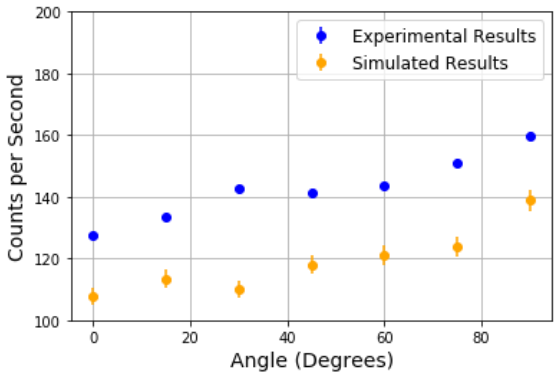

Figure 7. Comparison of the simulated and experimental results from detector inside of the borated polyethylene "house."

After determining that the simulation results from the "house" setup came within 20% of the experimental results, another experiment was run with the detector vertically inserted into the two LANL shielding designs. The M196 source was placed 25" from the center of the shielding window while the M797 source was rotated about the detector's center in increments of 15°. This setup is picture in Figure 4. This experiment was performed twice: once with each shielding design for a runtime of 120 seconds for each angle. The results from these two experiments are shown in Figures 8a and 8b.

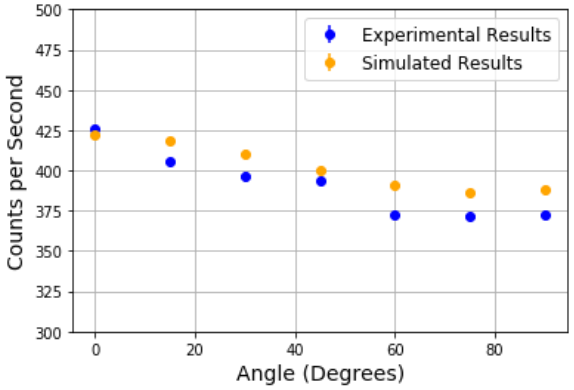

Figure 8a. Comparison of the simulated and experimental results from the shielding configuration with HDPe on the outer layer.

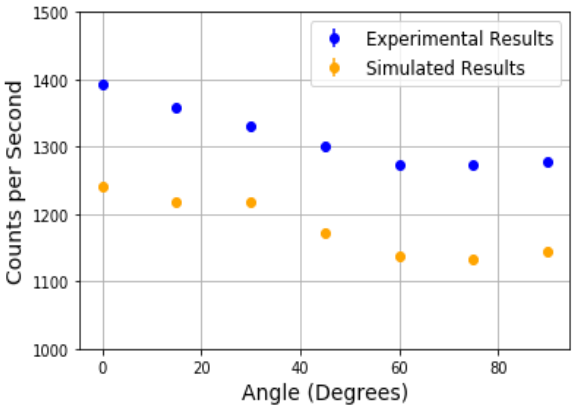

Figure 8b. Comparison of the simulated and experimental results from the shielding configuration with borated polyethylene on the outer layer.

The uncertainty bars from the simulated results result from the uncertainty given to all tally results calculated in MCNP, with error propagation for the uncertainty in each source strength accounted for. This source strength uncertainty was set to 2.5% based on the source strength uncertainty of similar sources [9]. This does not resolve all sources of uncertainty in the simulation results, and the actual uncertainty of these measurements is higher than shown in the graphs. However, other sources of uncertainty such as an inhomogeneous neutron source or anisotropic neutron emission were not accounted for because their exact characteristics are not known. When considering these uncertainties, the comparison for all three simulations fell within the desired 20% range from the experimental

results. The trend of the simulations as the angles increase also follows that of the experimental measurements.

4. Conclusion

The neutron measurements performed in this research provided a useful benchmark for refining the ^{10}B/ZnS(Ag) detector as well as valuable insight into the effectiveness of the two directional shield designs. The shield with an outer layer of high-density polyethylene was found to be more successful at limiting the counting contributions from sources outside of the area in front of the shield window due to the moderation provided by the HDPe, which increased the likelihood of absorption in the inner cadmium and borated polyethylene layers. However, the shield was not able to reduce the counts from both sources back to those recorded with just one source. This indicates that the thickness of the outer HDPe layer should be increased in order to further thermalize the fast neutrons coming from the sources.

The MCNP model of the ^{10}B/ZnS(Ag) was within 20% of the experimentally measured neutron count rates in each of the different shielding setups and for each different source location. Furthermore, the results from the MCNP simulations followed the trends in count rate that were observed in the experimental measurements as the second source was moved around the detector.

Going forward, the MCNP model of the ^{10}B/ZnS(Ag) detector will be used to help determine the optimal thicknesses of the layers in the directional shielding design to further minimize counting contributions from outside sources. Furthermore, more complex arrangements of sources will be introduced in the model to simulate the high radiation environments found in the waste storage rooms at Los Alamos National Laboratory.

This shield also has potential applications for remote radiological surveys of areas with high levels of radiation, allowing for less exposure for radiological workers. Measurements taken by the shielded detector in environments harmful to humans can be verified with the simulated detector rather than by human inspection.

Acknowledgements: *The authors would like to acknowledge that part of the research done is within the Los Alamos National Laboratory project 6L0000. LA-UR-21-29103.*

References

1. *Neutron Detector Suitable for Second Line of Defense Program*, Bridgeport Instruments LLC, Austin, TX, USA, 2020.
   Retrieved from: http://bridgeportinstruments.com/products/neutron/ndet_2x24_r1.pdf
   Retrieved on: August 20, 2021.
2. P. A. Söderström et al., "Characterization of a Plutonium-Beryllium Neutron Source," *Applied Radiation and Isotopes,* vol. 167, article no. 109441, Jan. 2021. https://doi.org/10.1016/j.apradiso.2020.109441
   PMID: 33002762
3. S. F. Mughabghab, *Thermal Neutron Capture Cross Sections Resonance Integrals and G-Factors*, Rep. INDC(NDS)-440, IAEA, Vienna, Austria, 2003.
   Retrieved from: https://inis.iaea.org/collection/NCLCollectionStore/_Public/34/020/34020739.pdf?r=1
   Retrieved on: Sep. 17, 2021
4. K. Guzman-Garcia et al., "10B+ZnS(Ag) as an Alternative to 3He-Based Detectors for Radiation Portal Monitors," *EPJ Web of Conferences*, vol. 153, article no. 07008, 2017. https://doi.org/10.1051/epjconf/201715307008
5. *Atlas of Neutron Capture Cross Sections*, Evaluated Data Library, IAEA, Vienna, Austria, 2010.
   Retrieved from: https://www.iaea.org/resources/databases/atlas-of-neutron-capture-cross-sections
   Retrieved on: August 20, 2021
6. *Compendium of Material Composition Data for Radiation Transport Modeling*, Rep. 200-DMAMC-128170 PNNL-15870, Rev. 2, Pacific Northwest National Laboratory, Richland, WA, USA, Apr. 2021.
   Retrieved from: https://www.pnnl.gov/main/publications/external/technical_reports/PNNL-15870Rev2.pdf
   Retrieved on: August 20, 2021
7. W.B. Wilson et al., *SOURCES 4A: A Code for Calculating (α, n), Spontaneous Fission, and Delayed Neutron sources and Spectra*, Rep. LA-13639-MS, Los Alamos National Laboratory, Los Alamos, New Mexico, USA, 1999. https://doi.org/10.2172/15215
8. J. K. Shultis., R. E. Faw, *An MCNP Primer*, Kansas State University, Manhattan, KS, USA, 2011.
   Retrieved from: https://www.mne.k-state.edu/~jks/MCNPprmr.pdf
   Retrieved on: August 20, 2021
9. M.S. Dewey, H.P. Mumm, "Calibrations: Neutron Source Strength," National Institute of Standards and Technology, U.S. Department of Commerce, Gaithersburg, MD, USA 2010.
   Retrieved from: https://www.nist.gov/programs-projects/calibrations-neutron-source-strength
   Retrieved on: November 18, 2021
10. H.R. Vega-Carrillo et al. "Characterization of a ^{239}PuBe Isotopic Neutron Source," in *Proceedings of the ISSSD*, IAEA, Vienna, Austria, 2012.
    Retrieved from: https://inis.iaea.org/collection/NCLCollectionStore/_Public/44/026/44026243.pdf
    Retrieved on: November 18, 2021